

Effects of Redistribution with Dipole Scattering on Line Source Functions

A. Peraiah and K. E. Rangarajan *Indian Institute of Astrophysics, Bangalore 560034*

Received 1981 March 20; accepted 1981 August 27

Abstract. The partial frequency redistribution function for zero natural line width with dipole scattering (R_1) has been considered in obtaining the simultaneous solution of the statistical equilibrium and line transfer equations in the comoving frame of the expanding gas. We have considered a non-LTE two level atom in an expanding spherical medium whose outer radii are 3, 10 and 20 times the stellar radius with a total optical depth $T \simeq 2 \times 10^3$. In all the cases, we have calculated the population ratio of the two levels N_2/N_1 and compared these results with those obtained by using different expansion velocities and geometrical extensions. Initially, the upper level population (N_2) is set equal to zero. The converged simultaneous solution shows that the upper level population is enhanced considerably from the initial value. Variation in velocity gradients seem to have little effect on the ratio N_2/N_1 when the geometrical thickness of the medium is 3 or 10 times the stellar radius. However, when the thickness is increased to 20 times the central radius, the velocity gradients change the ratio N_2/N_1 considerably in the region where $\log T \leq 2$. The effect of variation of geometrical thickness is to reduce the N_2/N_1 ratio at $\tau = 0$.

Key words: partial frequency redistribution—dipole scattering—statistical equilibrium equation—line transfer equation in the comoving frame.

1. Introduction

In an earlier paper (Peraiah 1980b, hereafter referred to as Paper I), we have investigated the simultaneous solution of the equation of radiative transfer and the statistical equilibrium equation. In this paper, we have treated the complete redistribution in a resonance line. Convergence was achieved within a small number of iterations. Complete redistribution was used for the sake of simplicity and to test the

capabilities of the method of obtaining the solution by direct iteration between the two equations. A considerable amount of work was done in calculating the lines in a fast expanding atmosphere using partial frequency redistribution in the comoving frame (see Mihalas, Kunasz and Hummer 1976; Peraiah 1980a). However, these calculations do not give a simultaneous solution of radiative transfer equation and statistical equilibrium equation. It is important that one must obtain a consistent solution for correct estimation of the line profiles. This becomes particularly obvious in the light of the calculations of Shine, Milkey and Mihalas (1975a,b) who simulated the centre to limb variation of solar Ca II H and K lines.

We intend to obtain a consistent solution using partial frequency redistribution with zero natural line width. We have considered isotropic and dipole scattering. The results of isotropic scattering are published elsewhere and the results of the calculations with dipole scattering are presented here. We have assumed a highly scattering medium with no continuum emission.

2. Outline of the computational procedure

The method is described in Paper I and we shall repeat the main points of the procedure. The statistical equilibrium equation for a two level atom is written as,

$$N_1 \left[B_{12} \int_{-\infty}^{+\infty} dx \phi(x) J_x + C_{12} \right] = N_2 \left[A_{21} + C_{21} + B_{21} \int_{-\infty}^{+\infty} dx \phi(x) J_x \right] \quad (1)$$

where N_1, N_2 are the number densities in the lower and upper levels, and B_{12}, B_{21} and A_{21} are the Einstein coefficients. C_{12} and C_{21} are the rates of the collisional excitation and de-excitation respectively. We have estimated these quantities for Hydrogen Lyman alpha line using the equations given by Jefferies (1968). J_x is the mean intensity at the normalized frequency, $x (\equiv (\nu - \nu_0)/\Delta_s, \Delta_s$ being a standard frequency interval). $\phi(x)$ is the profile function given by

$$\phi(x) = \int_{-\infty}^{+\infty} R(x, x') dx' \quad (2)$$

where $R(x, x')$ is the angle averaged partial redistribution function. In the case of zero natural line width (R_I) and dipole scattering, R is given by (see Hummer 1962, Peraiah 1978)

$$R_{I-AD}(x, x') = \frac{3}{8} \left\{ \frac{1}{\sqrt{\pi}} \int_{|x|}^{\infty} \exp(-t^2) dt [3 + 2(x^2 + x'^2) + 4x^2 x'^2] - \frac{\exp(-\bar{x}^2)}{\sqrt{\pi}} |\bar{x}| (2|x|^2 + 1) \right\}, \quad (3)$$

where \bar{x} and \underline{x} are the maximum and minimum values of x and x' . The profile is normalised such that

$$\int_{-\infty}^{\infty} \phi(x) dx = 1. \quad (4)$$

The statistical equilibrium equation will supply N_1 and N_2 and these are used to calculate the absorption at the line centre given by

$$K_L(r) = \frac{h \nu_0}{4\pi \Delta_s} (N_1 B_{12} - N_2 B_{21}). \quad (5)$$

The absorption coefficient given above is used in the calculation of J_x from the radiative transfer equation in the comoving frame

$$\begin{aligned} \mu \frac{\partial I(x, \mu, r)}{\partial r} + \frac{1 - \mu^2}{r} \frac{\partial I(x, \mu, r)}{\partial \mu} \\ = K_L(r) [\beta + \phi(r)] [s(x, r) - I(x, \mu, r)] \\ + \left\{ (1 - \mu^2) \frac{V(r)}{r} + \mu^2 \frac{dV(r)}{dr} \right\} \frac{\partial I(x, \mu, r)}{\partial x} \end{aligned} \quad (6)$$

and

$$\begin{aligned} -\mu \frac{\partial I(x, -\mu, r)}{\partial r} - \frac{1 - \mu^2}{r} \frac{\partial I(x, -\mu, r)}{\partial \mu} \\ = K_L(r) [\beta + \phi(r)] [S(x, \mu) - I(x, -\mu, r)] \\ + \left\{ (1 - \mu^2) \frac{V(r)}{r} + \mu^2 \frac{dV(r)}{dr} \right\} \frac{\partial I(x, -\mu, r)}{\partial x} \end{aligned} \quad (7)$$

where $I(x, \mu, r)$ is the specific intensity making an angle $\cos^{-1} \mu$ with the radius at r . β is the ratio of absorption per unit frequency interval in the continuum to that in the line centre. $V(r)$ is the velocity of the gas at the radial point r . $S(x, r)$ is the source function given by

$$S(x, r) = \frac{\phi(x)}{\beta + \phi(x)} S_L(r) + \frac{\beta}{\beta + \phi(x)} S_C(r). \quad (8)$$

Here $S_C(r)$ is the continuum source function and $S_L(r)$ the line source function given by

$$S_L(r) = \frac{(1 - \epsilon)}{\phi(x)} \int_{-\infty}^{+\infty} R(x, x') J(x') dx' + \epsilon B(r) \quad (9)$$

where $B(r)$ is the Planck function and ϵ is the probability per scattering, that a photon is lost by collisional de-excitation. The line source function can also be calculated from the level populations and is given by the formula

$$S_L(r) = \frac{A_{21} N_2(r)}{B_{12} N_1(r) - B_{21} N_2(r)} \quad (10)$$

We have set $\beta = 0$ and $S_C(r) = B(r)$ the Planck function, the initial radius to be 10^{12} cm and the geometrical extension is put equal to 3×10^{12} cm, 10^{13} cm and 2×10^{13} cm. The electron density is chosen to be varying as $1/r^3$ and initially at $r = 10^{12}$ cm, it is taken to be 10^{12} cm $^{-3}$. A constant temperature of 30,000 K is assumed in all the cases. We started the first iteration by assuming that all the neutral atoms are in the level 1 (*i.e.* $N_2 = 0$). This enables us to calculate the absorption coefficient in equation (5) with which we solve the line transfer given in equations (6) and (7). This solution is used to calculate the mean intensities J_x which can be inserted in equation (1) to obtain the new ratio of N_2/N_1 . This process is repeated until convergence is obtained within 1 per cent of N_2/N_1 in two successive iterations at each radial point.

We have considered the variation of density and velocity so that the equation of continuity is always satisfied in a spherically symmetric steady state flow. The velocity is changing with a negative gradient with respect to the optical depth. As we have divided the medium into 30 shells of equal geometrical thickness, the velocity gradient becomes a function of the absorption characteristics of the shell in question.

3. Discussion of the results

As we are calculating the solution of radiative transfer in the comoving frame, we need to calculate the partial frequency redistribution function only once. In Fig. 1,

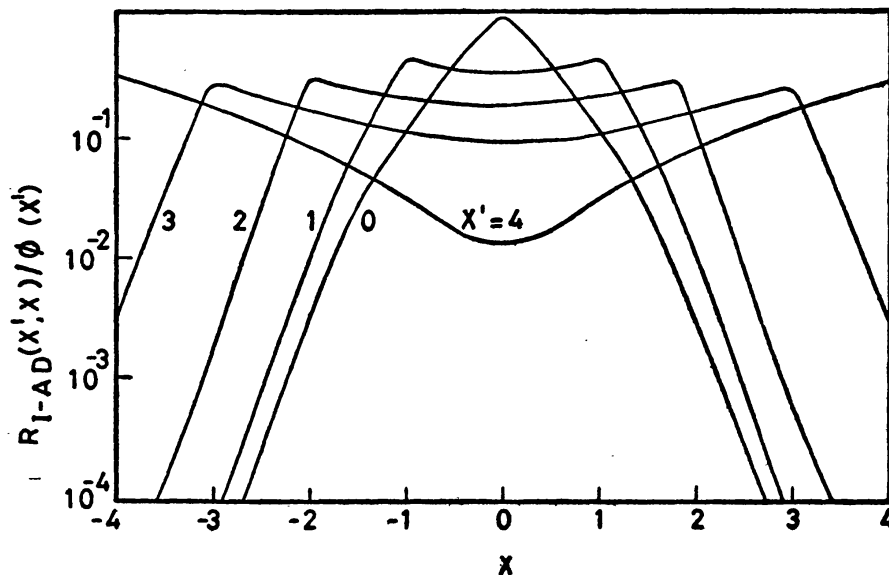


Figure 1. The probability of emission at frequency x per absorption at x' , $R_{I-AD}(x', x)/\phi(x')$ is given against x .

we have plotted $R_{I-AD}(x', x)/\phi(x')$ for x' , where the numerator is given by equation (3) and the denominator by equation (2). If we compare the probability of emission/absorption curves in this figure with those of Mihalas (1978, Figure 13-2, page 428) it becomes immediately obvious that there are important differences between these

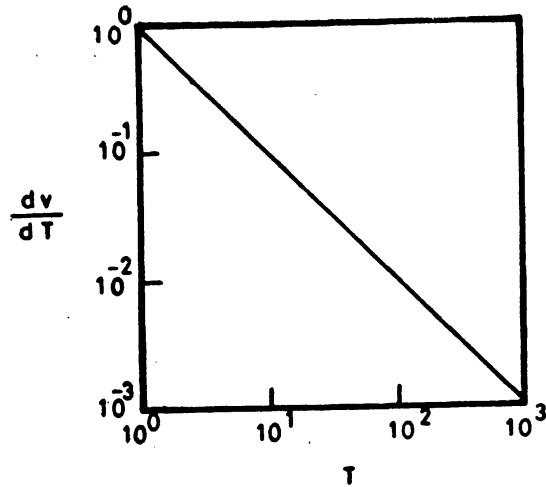


Figure 2. $dV/d\tau$, the velocity gradient with respect to optical depth is plotted against optical depth T .

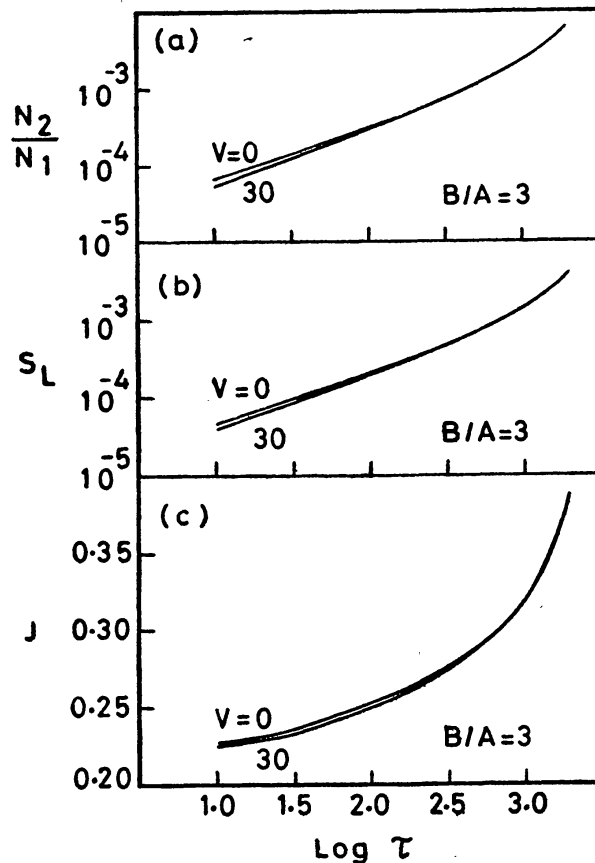


Figure 3. (a) The ratio of number densities of upper to lower level N_2/N_1 , (b) the line source function S_L and (c) the total mean density J are plotted against optical depth T for $B/A = 3$.

two results. These differences are mainly due to the type of scattering we have considered. Mihalas (1978) has used the expression for isotropic scattering whereas we have considered dipole scattering. For $x' = 0$, we note that the probability of finding a photon at $x = 0$ is nearly 1 in both the cases. As x' is increased, the probability flattens and becomes constant around $x = 0$ for isotropic scattering. However, the probability of finding the scattered photon around $x = 0$ reduces considerably for dipole scattering and at $x' = 4$, there is a clear dip in the curve. This difference between isotropic scattering and dipole scattering is quite important when we calculate the redistribution of photons from the line centre to the wings and vice versa in spherically symmetric expanding media.

In Fig. 2, we have given the velocity gradient versus the total optical depth. The velocity gradient is proportional to the total optical depth T , the optical depth being measured 0 at $r = r_{\max}$. This means that the velocity will be increasing with radius starting with $V(\tau = T) = 0$ and $V(\tau = 0) = V_{\max}$. We have set $V_{\max} = 0, 5, 10, 30$ mean thermal units (hereafter we need not mention mean thermal units).

In Fig. 3 (a, b, c) we have plotted the ratio N_2/N_1 , the line source function S_L and the total mean intensity J versus the total optical depth. The curves for various V_{\max} ($= 0, 5, \dots, 30$) cannot be resolved graphically and, therefore, we have presented results only for $V_{\max} = 0$ and 30. In this figure we have considered $B/A = 3$ (the ratio

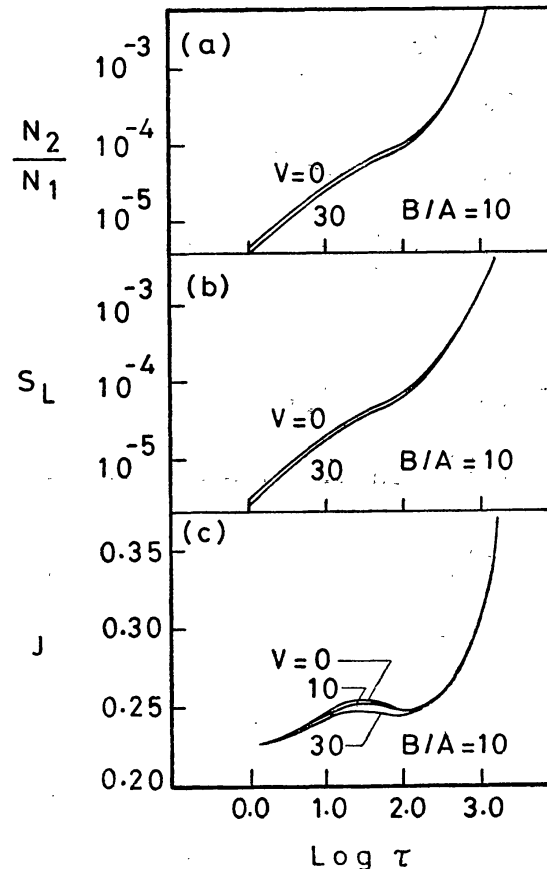


Figure 4. (a) The ratio of number densities of upper to lower level N_2/N_1 , (b) the line source function S_L and (c) the total mean intensity J are plotted against optical depth T for $B/A = 10$.

of outer to inner radii of the medium). We see that at $\tau = T$, the variation in velocity makes no difference either in the ratio N_2/N_1 or S_L or J . The changes in the above quantities are noticed only from $\log T \leq 2.5$. The change in N_2/N_1 from B to A is nearly two orders of magnitude whereas the source functions do not fall as rapidly. The ratio N_2/N_1 is much less than the equilibrium value even at the point $\tau = T$. The line source function and the ratio N_2/N_1 are reduced considerably mainly because of the fact that we have set $\beta = 0$ (i.e. no continuum emission) and the quantity ϵ is of the order of 10^{-6} to 10^{-8} . All the photons incident at $\tau = T$ are being scattered several times inside the medium. In particular at $\tau = T$, many of these are back scattered and consequently we notice that the source functions reduce at $\tau = 0$. These results look quite similar to those obtained in Paper I, in which we have employed complete redistribution (CRD). The fall in the ratio N_2/N_1 and S_L is more rapid in the case of partial frequency redistribution (PRD) than in the case of CRD. We needed a maximum velocity of 60 to obtain any graphically distinguishable results in the case of CRD whereas in PRD a maximum velocity of 30 is enough to get graphically resolvable results from those of $V_{\max} = 0$. We have plotted the ratio N_2/N_1 , S_L and J in Figs. 4 and 5 for $B/A = 10$ and 20 respectively. These are quite similar to those described in Fig. 3. The changes in N_2/N_1 for $B/A = 10$ are quite substantial. The changes in N_2/N_1 and S_L between the points A and B

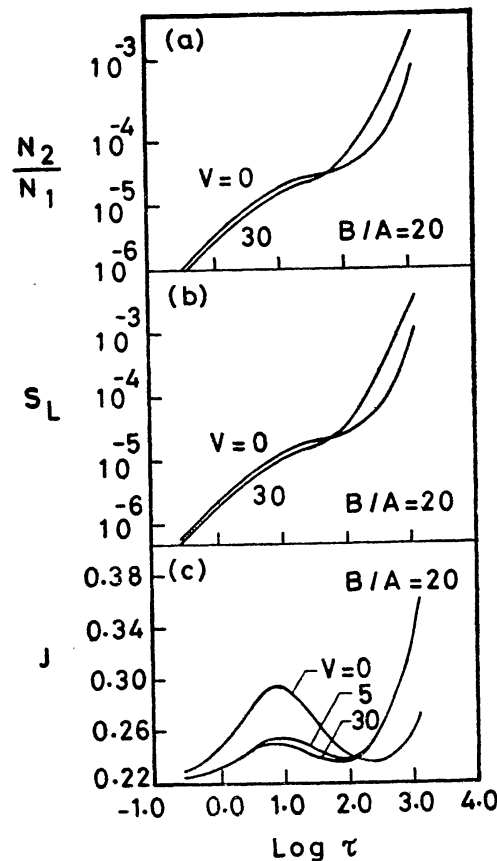


Figure 5. (a) The ratio of number densities of upper to lower level N_2/N_1 , (b) the line source function S_L and (c) the total mean intensity J are plotted against optical depth T for $B/A = 20$.

are as large as 4 to 5 orders of magnitudes. Most of the photons are involved in the multiple scattering at $\tau = T$ and consequently the radiation field is much more diluted than in the case of the medium with $B/A = 3$ or 10.

References

- Hummer, D. G. 1962, *Mon. Not. R. astr. Soc.*, **125**, 21.
Jefferies, J. T. 1968, *Spectral line formation*, Blaisdel, Waltham.
Mihalas, D. 1978, *Stellar Atmospheres*, 2nd edn., Freeman, San Francisco.
Mihalas, D., Kunasz, P. B., Hummer, D. G. 1976, *Astrophys. J.*, **210**, 419.
Peraiah, A. 1978, *Kodaikanal Obs. Bull. Ser. A.*, **2**, 115.
Peraiah, A. 1980a, *J. Astrophys. Astr.*, **1**, 3.
Peraiah, A. 1980b, *J. Astrophys. Astr.*, **1**, 101, (Paper I).
Shine, R. A., Milkey, R. W., Mihalas, D. 1975a, *Astrophys. J.*, **199**, 724.
Shine, R. A., Milkey, R. W., Mihalas, D. 1975b, *Astrophys. J.*, **201**, 222.